Electronic structures of *A*- and *B*-type DNA crystals

Masateru Taniguchi* and Tomoji Kawai
Nanoscience and Nanotechnology Center, The Institute of Scientific and Industrial Research, Osaka University, Osaka 567-0047, Japan
(Received 2 February 2004; published 29 July 2004)

The electronic band structures and total density of states based on a density-functional theory are performed on four deoxyribonucleic acid (DNA) molecules: namely, *A*- and *B*-type DNA where a single pitch is formed by 11 and 10 base pairs, respectively, of Poly(dA)·Poly(dT) and Poly(dG)·Poly(dC). Poly(dA)·Poly(dT) is a DNA where one single strand consists only of adenine (A) and the other single strand consists only of thymine (T), while Poly(dG)·Poly(dC) is a DNA where one single strand consists only of guanine (G) and the other of cytosine (C). *A*- and *B*-Poly(dA)·Poly(dT) and *A*- and *B*-Poly(dG)·Poly(dC) DNA. Compared in the same structure, the band gap of Poly(dA)·Poly(dT) is larger than that of Poly(dG)·Poly(dC). The highest occupied molecular orbitals (HOMO's) of Poly(dA)·Poly(dT) and Poly(dG)·Poly(dC) are formed by adenine's and guanine's HOMO, respectively, regardless of the structure type. On the other hand, the lowest unoccupied molecular orbitals (LUMO's) of DNA of both types are formed by the orbitals of Na and PO_4, though the LUMO's of *B*-Poly(dA)·Poly(dT) and *B*-Poly(dG)·Poly(dG) are formed by thymine's and cytosine's LUMO when the DNA-DNA distance is more than 3 nm. The minimum energy gap between the valence edge and the empty state of Na and PO_4 is 0.9 eV in *A*-Poly(dG)·Poly(dC). The narrow bandwidth of the valence and conduction bands show that the conduction arises not from band transport but a hopping mechanism in the presence of doping.

DOI: 10.1103/PhysRevE.70.011913 PACS number(s): 87.14.Gg, 87.15.Aa

I. INTRODUCTION

The electric conduction property of DNA has attracted much attention because of the one-dimensional layered structure of π-electron base molecules, and it has been measured by various methods. During initial stages, the electric conduction in DNA was studied by measurements of photoinducted electron transfer velocity in a donor-DNA-acceptor molecule, which was synthesized by modifying one edge of DNA with an electron-providing donor molecule and the other edge with an electron-absorbing acceptor molecule as performed by Barton and co-workers [1]. However, no unified view of the conduction in DNA can be obtained from arguments based on the electronic transfer theory [2–5]. Recent progress in superfine technology, on the other hand, has enabled us to construct nanoelectrodes with a spacing of molecular size and to measure electric conduction in a single DNA molecule or a DNA molecular bundle [6–12]. However, the reported DNA conduction properties range from insulator [8–10] to metal [11,12] and the nanoscale measurements did not fully clarify the electric conduction property of DNA [13]. The discrepancy in the experimental results is attributed to the diversity of the DNA structure, base sequence, and experimental atmosphere used in the experiments and therefore we cannot simply compare the results.

The electronic state of DNA is expected to depend on the structure, base sequence, measurement atmosphere, and measurement method [14]. Among these, the structure and base sequence would greatly influence the electronic state. Poly(dA)·Poly(dT) and Poly(dG)·Poly(dC), having the simplest base sequence, have a phase transition from *B*-type structure to *A*-type structure, as the relative humidity and salt concentration decrease [15–17]. The *A*- and *B*-type structures are different in the overlapping manner [18,19] of the base molecules and hence their electronic states are expected to be different. Felice *et al.* [18] and Maragakis *et al.* [20] pointed out the modification of the electronic state due to the change of the base-molecule overlapping. However, the electronic state of *A*- and *B*-type DNA with the same base molecules is not yet fully clarified. The base-molecule dependence of the physical property was recently indicated by an experiment where iodine was doped in a vacuum into Poly(dA)·Poly(dT) and Poly(dG)·Poly(dC) that were fixed on the nanoelectrodes with a 30-nm spacing [21]. From this experiment, the electronic state of DNA was expected to change with the base-molecule sequence, although the state is not well understood.

In this paper, in order to investigate the influence of the base sequence and structure on the electronic states of DNA, we performed band calculations for *A*-Poly(dA)·Poly(dT), *A*-Poly(dG)·Poly(dC), *B*-Poly(dA)·Poly(dT), and *B*-Poly(dG)·Poly(dC) using the density-functional method. We considered all the molecules constituting DNA—i.e., base molecule, sugar, phosphoric acid, and sodium—because the conformation of the backbones and sodium is closely related to DNA structures.

II. METHODS AND MODELS

All calculations have been performed using the program DMOL [3] based on the density-functional theory [22]. The crystalline orbitals are extended as a linear combination of basis set consisting of atom-centered orbitals. The minimal basis sets were used for all atoms. The basis set orbitals are

*Corresponding author. Electronic address: taniguti@sanken.osaka-u.ac.jp

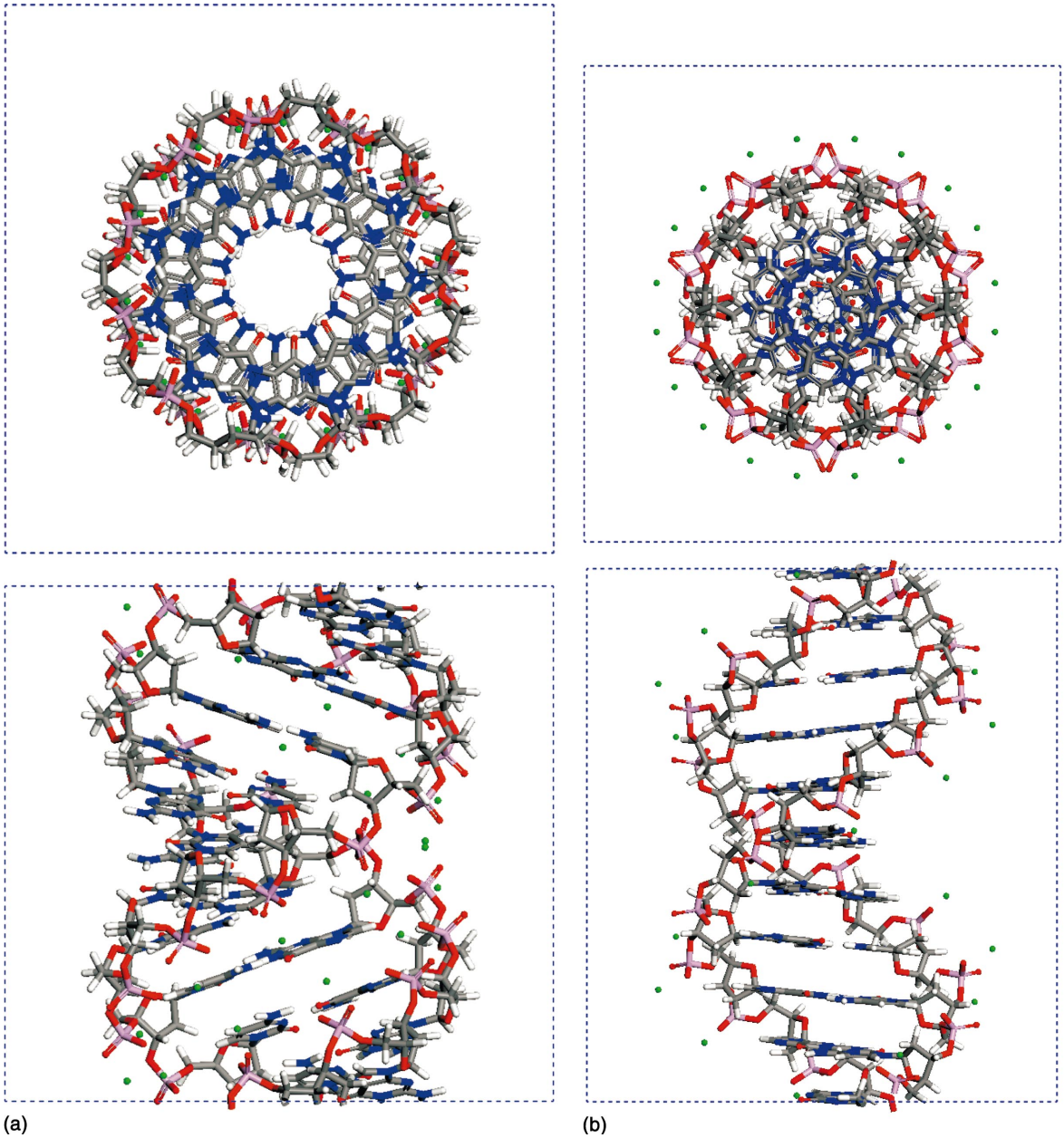

FIG. 1. (Color) Side and top views of the crystal structure of (a) *A*-type DNA and (b) *B*-type DNA with $a=3$ nm. The green dot shows the Na atom.

cut off at a radius of 5.5 Å. Effective core potentials were used for all core electrons. The Brillouin zone was sampled using $[1\times1\times36]$ Mokhorst-Pack [23] k points, which are characterized by divisions along three reciprocal space axes. When the mesh parameters of the a and b axes were increased, the electronic band structures and total density of states showed no change. Relaxation of total energy per cell was converged to 10^{-5} Ha. The generalized gradient approximation (GGA) was used; BLYP is constructed by combining the correlation functional of Lee, Yang, and Par (LYP) [24] with exchange functional of Becke [25]. The total charge was neutral and the spin multiplicity was singlet.

The calculation was conducted for the three-dimensional crystal structure where a unit cell contains a single pitch, as shown in Fig. 1. In this structure, DNA forms a double helix along the c axis. The unit cell is taken from the tetragonal system, the cell parameters are designated as $a(=b)=3$ nm, and the c-axis length is 28.2 Å for the *A*-type structure and 33.8 Å for *B*-type. *A*-type DNA has 11 base pairs in a pitch and hence, when moving to the next base pair, the height increases by 2.56 Å and the rotation angle by 32.7°. As viewed along the *C* axis, the sugar and phosphoric groups form outer circles and the base pairs form an inner circle in which there is an empty space of about 7.2 Å. In contrast, *B*-type DNA has ten base pairs in a pitch and hence, when moving to the next base pair, the height increases by 3.38 Å and the rotation angle by 36°. As viewed along the *C* axis of the *B*-type DNA, the sugar and phosphoric groups form outer circles and the base pairs form an inner circle where no empty space exists. The above-mentioned positions of sugar,

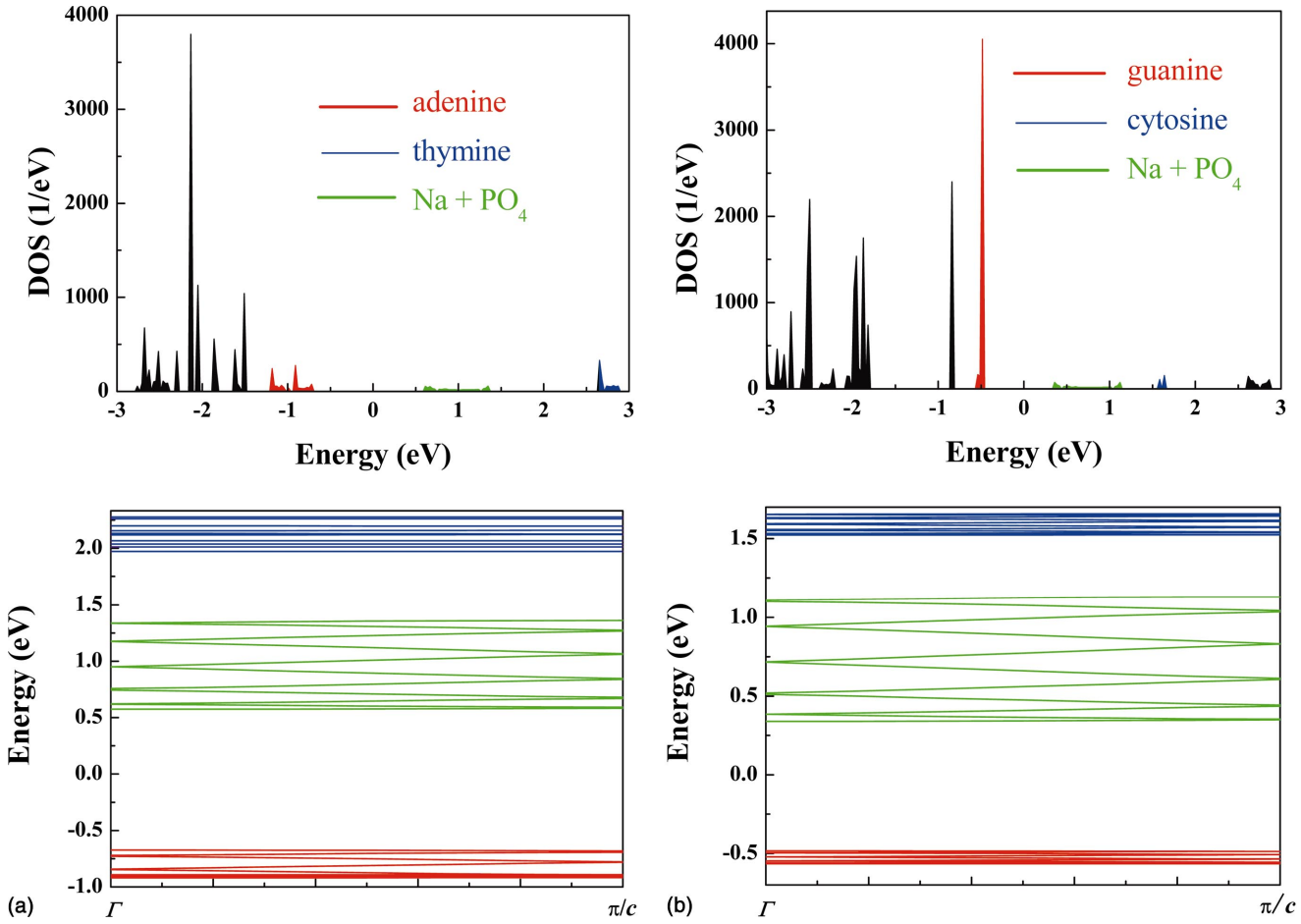

FIG. 2. (Color) Electronic band structures and total density of states of (a) *A*-Poly(dA)·Poly(dT) and (b) *A*-Poly(dG)·Poly(dC) with $a=3$ nm. The Fermi levels are set to 0 eV.

phosphoric acid, and base pairs were set by the INSIGHTII package. Structural optimization by means of molecular dynamics for a structure that includes base pairs, phosphoric acid, and sugar resulted in the cutting of hydrogen bonds between base pairs and the DNA structure could not be maintained. We therefore fixed the coordinates of base pairs, performed energy relaxation using molecular dynamics (DISCOVER) for the structures of phosphoric acid and sugar, and employed the obtained structure.

We determined the spatial configuration of Na by the B3LYP method [24,25] that combines Beck's three-parameter nonlocal exchange functional with the nonlocal correlation functional of Lee, Yang, and Parr using the base function 6-31G(d,p) [26] for the structural optimization of NaH_2PO_4. The position of Na is 2.2 Å away from the oxygen atom and the P-O-Na angle is 87.6°. Na lies on the perpendicular bisector of the base O-O of the isosceles triangle O-P-O. The calculated structural positions of Na and O are incorporated in the DNA structure based on the P atom locations. In our calculation model, *A*-Poly(dA)·Poly(dT), *A*-Poly(dG)·Poly(dC), *B*-Poly(dA)·Poly(dT), and *B*-Poly(dG)·Poly(dC) contain 473, 473, 430, and 430 heavy atoms and 253, 242, 230, and 220 hydrogen atoms, respectively. The chemical composition of those models is $C_{220}H_{235}N_{77}O_{132}P_{22}Na_{22}$, $C_{209}H_{242}N_{88}O_{132}P_{22}Na_{22}$, $C_{200}H_{230}N_{70}O_{120}P_{20}Na_{20}$, and $C_{190}H_{220}N_{80}O_{120}P_{20}Na_{20}$, respectively.

III. ELECTRONIC STRUCTURES OF *A*-TYPE DNA

The *A*-type structure is stable in a low ion concentration and low humidity [14–17]. The position of Na derived in the structural optimization of NaH_2PO_4 is incorporated in the DNA structure based on the phosphorus atom locations. The structure is shown in Fig. 1(a). The nearest-neighbor Na-Na distance in this structure is 3.31 Å, which is larger than the sum of the Na-ion radius (1.16 Å) [27]. The band structure and density of states of *A*-Poly(dA)·Poly(dT) and *A*-Poly(dG)·Poly(dC) for $a=3$ nm are shown in Figs. 2(a) and 2(b). Fermi levels are set to 0 eV in both cases. The valence bands in *A*-Poly(dA)·Poly(dT) and *A*-Poly(dG)·Poly(dC) are formed by adenine's highest occupied molecular orbital (HOMO) and by guanine's HOMO, respectively. Both valence bands consist of 11 bands. The conduction bands are formed by Na and phosphoric groups. The widths of the valence and conduction bands are respectively, given by 0.244 eV and 0.779 eV in *A*-Poly(dA)·Poly(dT) and 0.081 eV and 0.771 eV in *A*-Poly(dG)·Poly(dC). The band gap is 1.249 eV in *A*-Poly(dA)·Poly(dT) and 0.824 eV in *A*-Poly(dG)·Poly(dC).

There is a band formed by lowest unoccupied molecular orbital (LUMO) of thymine and cytosine, at 0.613 eV [*A*-Poly(dA)·Poly(dT)] or 0.393 eV [*A*-Poly(dG)·Poly(dC)] at a higher level from the conduction band. The band width is 0.360 eV in *A*-Poly(dA)·Poly(dT) and 0.133 eV in *A*-Poly(dG)·Poly(dC). Since the valence-band width in *A*-Poly(dG)·Poly(dC) is one-third of the width in *A*-Poly(dA)·Poly(dT), the valence band in *A*-Poly(dG)·Poly(dC) is less dispersive and therefore its density of states is extremely high. According to the molecular orbital calculation at the Γ point, the HOMO electron densities of *A*-Poly(dA)·Poly(dT) and *A*-Poly(dG)·Poly(dC) are mostly located on adenine and guanine, respectively, and π electrons extend over the base molecules, as given in Fig. 3(a). Since in the HOMO's of both DNA all the HOMO's of adenine and guanine have an antibonding interaction with each other, the transfer integral between the HOMO's of the base molecules is small and hence the band width at the valence band edge is only 7 meV in *A*-Poly(dA)·Poly(dT) and 3 meV in *A*-Poly(dG)·Poly(dC). The electron density of the LUMO, on the other hand, is located on the Na and phosphoric groups and extends mostly over Na, as given in Fig. 3(b). The molecular orbital calculation at the Γ point for the LUMO band of thymine shows that the electron density is accumulated on several of the 11 thymine molecules. Hence, although the width is 0.36 eV, the band is almost dispersionless, forming a flat band. In contrast, the LUMO band of cytosine molecules is narrow but dispersive.

In our models of both *A*-Poly(dA)·Poly(dT) and *A*-Poly(dG)·Poly(dC), there are bands of Na and phosphoric groups between the π-electron bands of the base molecules. Gervasio *et al.* [28] pointed out that the energy levels of the Na and phosphoric groups could lie in between the base-pair-formed bands. Essentially, do the bands of the Na and phosphoric groups always lie in between the π-electron bands of the base molecules? To clarify this, we first performed the band calculation designating the *a*-axis length as 2.5 nm and 10 nm. Although there was a slight change in the band gap, the relative positions of the levels of the base molecules, Na, and the phosphoric group in the band structure and the band width did not change at all. Also the Mulliken charge of Na was +0.8 and did not show any dependence on the unit cell size and the electronic state of Na did not change with the unit cell—i.e., the distance between DNA. Therefore, we conclude that the *A*-type DNA has no orbital interaction between DNA chains and the Na and PO_4 bands always lie in between the bands of the base molecules in this model structure.

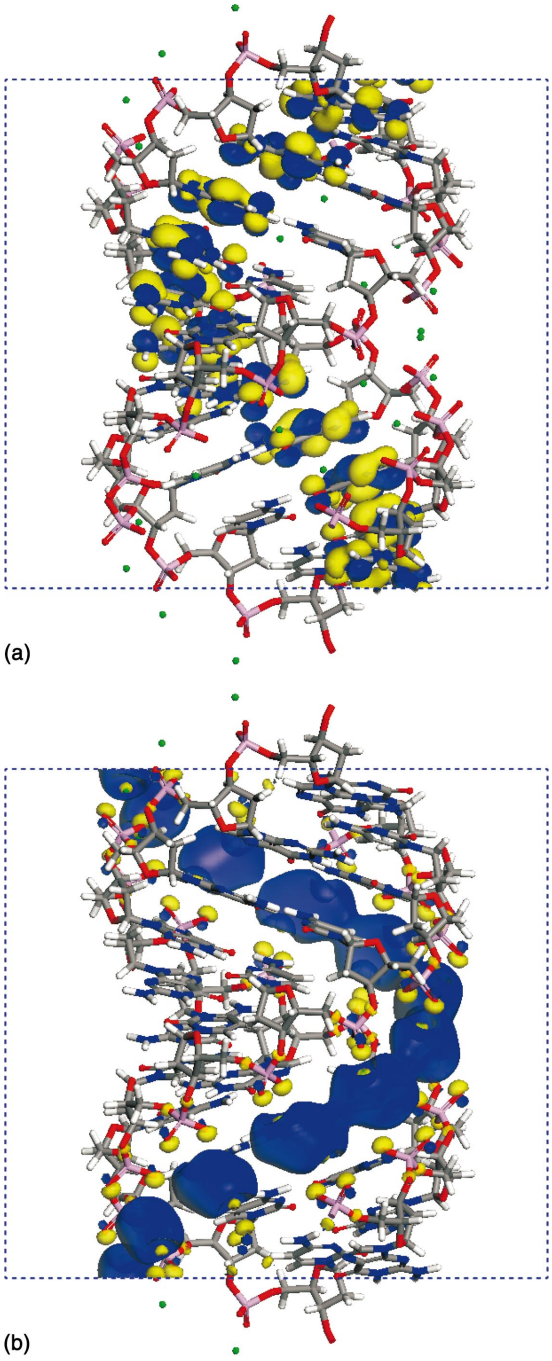

FIG. 3. (Color) Side views of the isosurface plot of (a) the HOMO and (b) the LUMO of *A*-Poly(dG)·Poly(dC) with $a=3$ nm at the Γ point. The blue and yellow isosurfaces show positive and negative isovalues, respectively. The isosurfaces have a value of 0.01.

IV. ELECTRONIC STRUCTURES OF *B*-TYPE DNA

The *B*-type is a typical DNA structure that most easily suffers from environmental change [14–17]. When $a=3$ nm, the *B*-type structure has a form shown in Fig. 1(b) where the Na-Na nearest-neighbor distance is 9.07 Å, about 3 times as long as that of the *A*-type DNA. In the *A*-type, the Na ion is located in the channel formed by the DNA, while in the *B*-type, it lies in the outermost part. The band structures of *B*-Poly(dA)·Poly(dT) and *B*-Poly(dG)·Poly(dC) are shown in Figs. 4(a) and 4(b). The Fermi level is set at 0 eV. The valence band of *B*-Poly(dA)·Poly(dT) is formed by adenine's HOMO and the conduction band by thymine's LUMO. On the other hand, the valence and conduction bands of *B*-Poly(dG)·Poly(dC) are formed, respectively, by guanine's HOMO and cytosine's LUMO. The band widths of the valence and conduction bands are, respectively, 0.045 eV

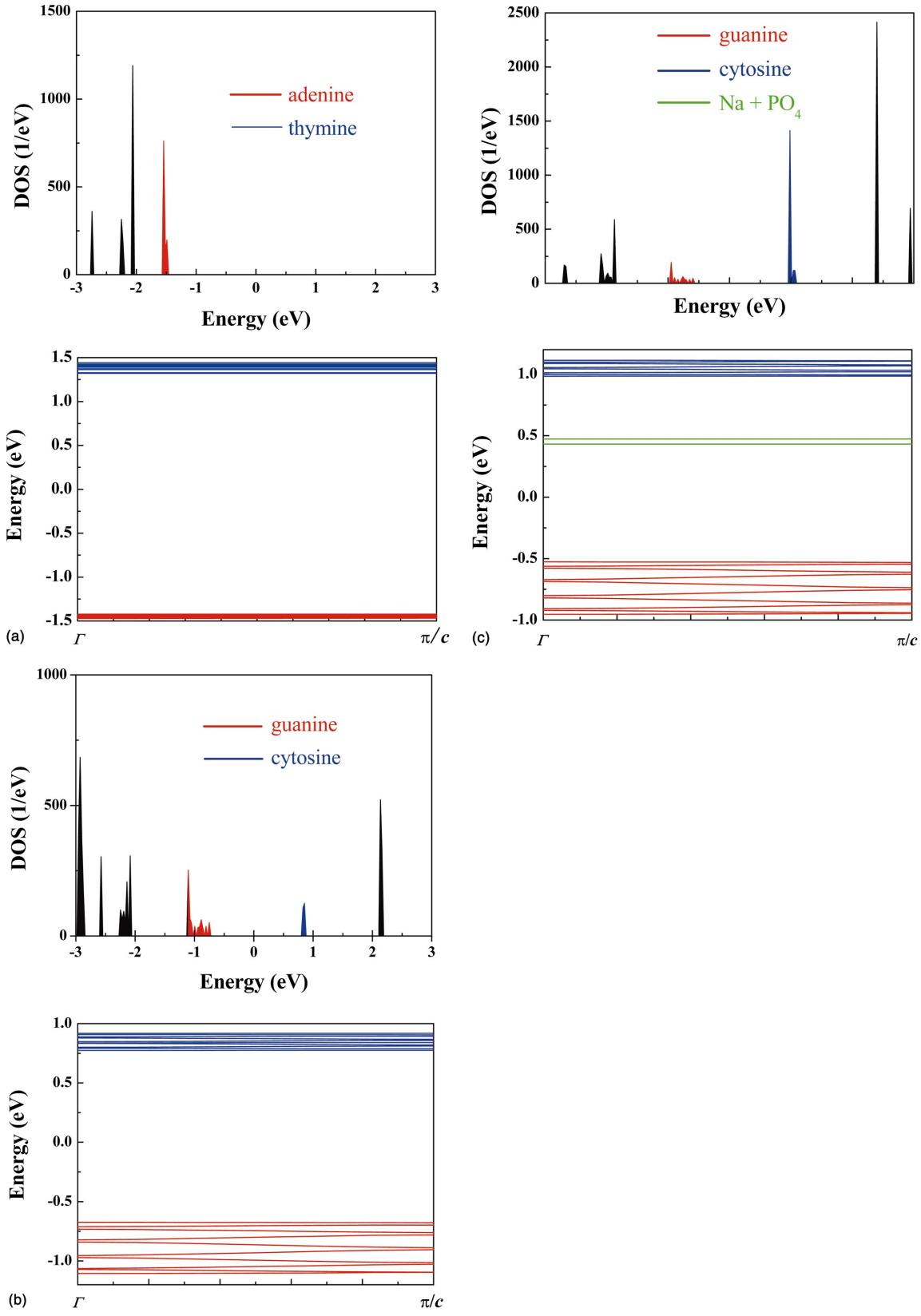

FIG. 4. (Color) Electronic band structures and total density of states of (a) *B*-Poly(dA)·Poly(dT) with $a=3$ nm, (b) *B*-Poly(dG)·Poly(dC) with $a=3$ nm, and (c) *B*-Poly(dG)·Poly(dC) with $a=2.5$ nm. The Fermi levels are set to 0 eV.

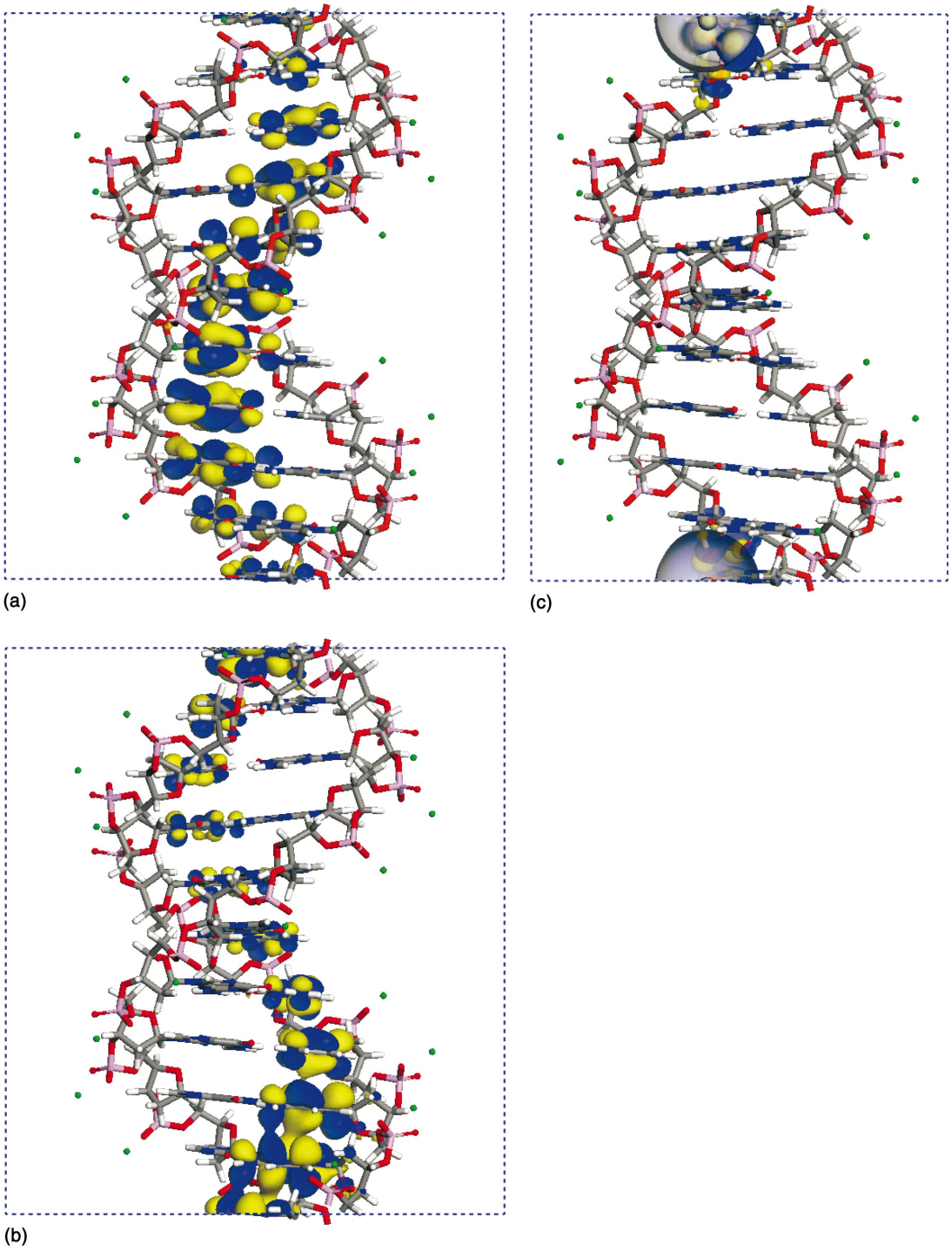

FIG. 5. (Color) Side views of the isosurface plot of (a) the HOMO and (b) the LUMO of *B*-Poly(dG)·Poly(dC) at the Γ point with $a=3$ nm, and (c) the LUMO with $a=2.5$nm. The blue and yellow isosurfaces show positive and negative isovalues, respectively. The isosurfaces have a value of 0.01.

and 0.120 eV in *B*-Poly(dA)·Poly(dT) and 0.421 eV and 0.143eV in *B*-Poly(dG)·Poly(dC). The band gap is 2.743 eV in *B*-Poly(dA)·Poly(dT) and 1.448 eV in *B*-Poly(dG)·Poly(dC). The band gap in *B*-Poly (dG)·Poly(dC) is the same as the one that Lewis *et al.* [29] obtained by a local density approximation (LDA) calculation.

The calculation of the HOMO at the Γ point in *B*-type DNA shows that the HOMO consists of HOMO's of adenine and guanine and the π electrons extend over the base mol-

TABLE I. Calculated band parameters of *A*- and *B*-type DNA with $a=3$ nm. Energies in eV. W_H, W_L, and W_{Na} show the band widths formed by the HOMO and LUMO of base molecules and the orbitals of Na and PO_4, respectively. ΔE is the band gap.

DNA	ΔE	W_H	W_L	W_{Na}
A-Poly(dA)·Poly(dT)	1.249	0.244	0.360	0.779
A-Poly(dG)·Poly(dC)	0.824	0.081	0.133	0.771
B-Poly(dA)·Poly(dT)	2.743	0.045	0.120	
B-Poly(dG)·Poly(dC)	1.448	0.421	0.143	

ecules, as given in Fig. 5(a). However, since the HOMO's in both DNA are formed from the state where all the HOMO's in the base molecules have an antibonding interaction with each other, the transfer integral between adenines or guanines is small and hence the band widths at the valence-band edge are only 1 meV in *B*-Poly(dA)·Poly(dT) and 4 meV in *B*-Poly(dG)·Poly(dC). The molecular orbital forming the conduction band, on the other hand, is the π-electron orbital composed of the LUMO of thymine or cytosine, as given in Fig. 5(b). Since the electron density in *B*-Poly(dA)·Poly(dT) is localized on some thymines, the density of states of the conduction band diverges.

In *A*-type DNA there are energy levels of Na and phosphoric acid lying in between the π-electron bands of base molecules, while there are no such levels in the *B*-type with $a=3$ nm. However, the calculation with $a=2.5$ nm indicated the appearance of localized levels of the Na and phosphoric groups between the π-electron bands, as given in Fig. 4(c). When $a=2.5$ nm, the energy gaps between the localized levels of the Na and phosphoric groups and the valence band are 1.904 eV in *B*-Poly(dA)·Poly(dT) and 0.957 eV in *B*-Poly(dG)·Poly(dC). The valence and conduction bands in this case are independent of the distance between DNA; however, the band gaps between the bands are 2.761 eV in *B*-Poly(dA)·Poly(dT) and 1.509 eV in *B*-Poly(dG)·Poly(dC), which are larger, respectively, by 18 meV and 61 meV than the gap when $a=3$ nm. The electron density of the LUMO at the Γ point is localized on some Na and phosphoric groups, as shown in Fig. 5(c). On the other hand, taking an *a*-axis length longer than 3 nm only slightly increases the band gap. In our model structure, *A*-type DNA has bands of Na and PO_4 between base-molecule-formed bands irrespective of the distance between DNA, while the localized levels of Na and PO_4 appear in *B*-type DNA depending on the DNA-DNA distance.

V. DISCUSSION

The density-functional-band calculation for *A*- and *B*-type Poly(dA)·Poly(dT) and Poly(dG)·Poly(dC) showed the different electronic structure for types *A* and *B*. The band parameters of *A*- and *B*-type DNA at $a=3$ nm are summarized in Table I. The band gap of the DNA estimated by the photoelectron spectroscopy measurement is about 4.5–5.0 eV [30], but usually, the band gap obtained from the density-functional-band calculation is smaller than the experimental value. We also performed calculations with a double-numerical base function to see the base function dependence and found that the HOMO-LUMO gap does not change from the value obtained using the minimal basis base function. Our calculation derived the same energy gap as in the result of Lewis *et al.* who used *ab initio* molecular dynamics [29]. This could be an effective method to combine molecular dynamics and DFT calculations in systems where van der Waals interactions play an important role as seen in DNA base pairs. However, as Bogar and Ladik reported, a band gap in such a system can be calculated close to the experimental data by introducing a virtual orbital (phantom atom) to expand the space between molecules [31,32]. Therefore, a better result can be expected if phantom atoms are introduced in the DMOL [3] that we used. If we compare the valence-band width of the base-molecule π electrons, the largest width is 0.421 eV found in *B*-Poly(dG)·Poly(dC) and the smallest is 0.045 eV in *B*-Poly(dA)·Poly(dT). Therefore, according to the valence-band width, the increase of the electric conductivity by doping holes in DNA can be most expected for *B*-Poly(dG)·Poly(dC). Let us consider a case of doping a single hole per unit cell. The doped holes would be located in the HOMO in DNA. Since the HOMO has a narrow band width under 10 meV, the doped holes are strongly localized and hence we expect an incoherent hopping conduction rather than a coherent conduction. In the case of electron doping, on the other hand, the highest increase of the electric conduction is expected for *A*-Poly(dA)·Poly(dT). As in the hole-doping case, the conduction could be due to hopping because of the narrow band width. Therefore, if doped DNA molecules show good conducting behavior, holes or electrons will have to couple to high-energy phonons such as molecular vibrations.

The energy gaps between the empty states of Na and PO_4 and the valence-band edge are less than 1.904 eV, and particularly the energy gap in *A*-Poly(dG)·Poly(dC) is a minimum value of 0.824 eV. It is expected that the small energy gap can create a carrier, which is excited at low energy. In the excited state, an electron is moved from the valence band to the band or local state of Na and PO_4. This result agrees with the conclusions of Gervasio *et al.* which show that electron transfer plays a dominant role in optical conductivity at low energy [28]. When the transition between the valence band and the empty state formed by Na and PO_4 can occur in four DNA molecules, there will be the difference between the optical conductivities.

VI. SUMMARY

We studied the influence of the structure and base sequence on the electronic state using the density-functional method. The valence bands in Poly(dA)·Poly(dT) and Poly(dG)·Poly(dC) are formed by the HOMO's of adenine and guanine, regardless of their structures. In the *A*-type

DNA, the bands of Na and PO_4 form a conduction band irrespective of the distance between DNA. In *B*-type DNA, localized levels of Na and PO_4 appear in the band gap only when the distance between DNA is small. From the band width, we expect that the electric conductivity would increase most by electron doping in *A*-Poly(dA)·Poly(dT) or by hole doping in *B*-Poly(dG)·Poly(dC). Because of the small band width, hopping conduction is indicated.

ACKNOWLEDGMENTS

We are grateful to Dr. Masashi Furukawa, Dr. Hiroyuki S. Kato, Dr. Maki Kawai, Dr. Takaki Hatsui, and Professor Nobuhiro Kosugi for photoelectron spectroscopy. This work was supported by the Center of Excellence (COE) program under the Ministry of Education, Science, Sports and Culture of Japan.

[1] C. J. Murphy, M. R. Arkin, Y. Jenkins, N. D. Ghatlia, S. H. Bossmann, N. J. Turro, and J. K. Barton, Science **262**, 1025 (1993); D. B. Hall, R. E. Holmlin, and J. K. Barton, Nature (London) **382**, 731 (1996); P. J. Dandliker, R. E. Holmlin, and J. K. Barton, Science **275**, 1464 (1997); M. Nunez, D. B. Hall, and J. K. Barton, Chem. Biol. **6**, 85 (1999); S. O. Kelley and J. K. Batron, Science **283**, 375 (1999).

[2] S. Priyadarshy, S. M. Risser, and D. N. Beratan, J. Phys. Chem. **100**, 17678 (1996).

[3] A. K. Felts, W. T. Pollard, and R. A. Friesener, J. Phys. Chem. **99**, 2929 (1995).

[4] E. J. C. Olson, D. H. Hormann, and P. F. Barbara, J. Phys. Chem. B **101**, 299 (1997).

[5] K. Fukui and K. Tanaka, Angew. Chem., Int. Ed. **37**, 158 (1998).

[6] D. Porath, A. Bezryadin, S. De Vries, and C. Dekker, Nature (London) **403**, 635 (2000).

[7] A. Rakitin, P. Aich, C. Papadopoulos, Y. Kobzar, A. S. Vedeneev, J. S. Lee, and J. M. Xu, Phys. Rev. Lett. **86**, 3670 (2001).

[8] A. J. Storm, J. van Noort, S. de Vries, and C. Dekker, Appl. Phys. Lett. **79**, 3881 (2001).

[9] E. Braun, Y. Eichen, U. Sivan, and G. Ben-Yoseph, Nature (London) **391**, 775 (1998).

[10] P. J. De Pablo, F. Moreno-Herrero, J. Colchero, J. G. Herrero, P. Herrero, A. M. Baró, P. Ordejón, J. M. Soler, and E. Atracho, Phys. Rev. Lett. **85**, 4992 (2000).

[11] A. Y. Kasumov, M. Kociak, S. Guéron, B. Reulet, V. T. Volkov, D. V. Klinov, and H. Bouchiat, Science **291**, 280 (2001).

[12] H. W. Fink and C. Schönenberger, Nature (London) **398**, 407 (1999).

[13] C. Dekker and M. A. Ratner, Phys. World **14**, 29 (2001).

[14] W. Saenger, *Principles of Nucleic Acid Structure* (Springer-Verlag, New York, 1984).

[15] S. Arnott and D. W. L. Hukins, Biochem. Biophys. Res. Commun. **47**, 1504 (1972).

[16] S. Arnott and E. Selsing, J. Mol. Biol. **88**, 551 (1974).

[17] G. Albiser, A. Lamiri, and S. Premilat, Int. J. Biol. Macromol. **28**, 199 (2001).

[18] R. D. Felice, A. Calzolari, and E. Molinari, Phys. Rev. B **65**, 045104 (2001).

[19] H. Sugiyama and I. Saito, J. Am. Chem. Soc. **118**, 8710 (1996).

[20] P. Maragakis, R. L. Barnett, E. Kaxiras, M. Elstner, and T. Frauenheim, Phys. Rev. B **66**, 241104 (2002).

[21] M. Taniguchi, H. Y. Lee, H. Tanaka, and T. Kawai, Jpn. J. Appl. Phys., Part 2 **42**, L215 (2003).

[22] B. Delley, J. Chem. Phys. **92**, 508 (1990); **94**, 7245 (1991).

[23] H. J. Monkhorst and J. D. Pack, Phys. Rev. B **13**, 5188 (1976).

[24] C. Lee, W. Yang, and R. G. Parr, Phys. Rev. B **37**, 785 (1988).

[25] A. D. Becke, Phys. Rev. A **38**, 3098 (1988); J. Chem. Phys. **98**, 5648 (1993).

[26] M. J. Frisch, G. W. Trucks, H. B. Schlegel, G. E. Scuseria, M. A. Robb, J. R. Cheeseman, V. G. Zakrzewski, J. A. Montgomery, Jr., R. E. Stratmann, J. C. Burant, S. Dapprich, J. M. Millam, A. D. Daniels, K. N. Kudin, M. C. Strain, O. Farkas, J. Tomasi, V. Barone, M. Cossi, R. Cammi, B. Mennucci, C. Pomelli, C. Adamo, S. Clifford, J. Ochterski, G. A. Petersson, P. Y. Ayala, Q. Cui, K. Morokuma, N. Rega, P. Salvador, J. J. Dannenberg, D. K. Malick, A. D. Rabuck, K. Raghavachari, J. B. Foresman, J. Cioslowski, J. V. Ortiz, A. G. Baboul, B. B. Stefanov, G. Liu, A. Liashenko, P. Piskorz, I. Komaromi, R. Gomperts, R. L. Martin, D. J. Fox, T. Keith, M. A. Al-Laham, C. Y. Peng, A. Nanayakkara, M. Challacombe, P. M. W. Gill, B. Johnson, W. Chen, M. W. Wong, J. L. Andres, C. Gonzalez, M. Head-Gordon, E. S. Replogle, and J. A. Pople, computer code GAUSSIAN98, revision A. 11.4, Gaussian, Inc., Pittsburgh, PA, 2002.

[27] R. D. Shannon and C. T. Prewitt, Acta Crystallogr., Sect. B: Struct. Crystallogr. Cryst. Chem. **25**, 925 (1969); R. D. Shannon, Acta Crystallogr., Sect. A: Cryst. Phys., Diffr., Theor. Gen. Crystallogr. **32**, 751 (1976).

[28] F. L. Gervasio, P. Carloni, and M. Parrinello, Phys. Rev. Lett. **89**, 108102 (2002).

[29] J. P. Lewis, P. Ordejón, and O. F. Sankey, Phys. Rev. B **55**, 6880 (1997).

[30] M. Furukawa, H. S. Kato, M. Taniguchi, T. Hatsui, N. Kosugi, T. Kawai, and M. Kawai (unpublished).

[31] F. Bogar and J. Ladik, Chem. Phys. **237**, 273 (1998); J. Mol. Struct.: THEOCHEM **501**, 445 (2000).

[32] J. Ladik, J. Mol. Struct.: THEOCHEM **544**, 1 (2001).